Journal of Organometallic Chemistry 694 (2009) 2597–2603

Contents lists available at ScienceDirect

Journal of Organometallic Chemistry

journal homepage: www.elsevier.com/locate/jorganchem

Lanthanide-centered inorganic/organic hybrids from functionalized 2-pyrrolidinone-5-carboxylic acid bridge: Covalently bonded assembly and luminescence

Bing Yan *, Hai-Feng Lu

Department of Chemistry, Tongji University, Siping Road 1239, Shanghai 200092, China

ARTICLE INFO

Article history:
Received 10 January 2009
Received in revised form 29 March 2009
Accepted 31 March 2009
Available online 14 April 2009

Keywords:
Organic–inorganic hybrids
Chemically bonded
Lanthanide ion
Photophysical property
Organometallic molecular hybrids

ABSTRACT

A series of organic–inorganic hybrid material with chemically bonding have been prepared through the precursor (PDCA-Si) derived from 2-pyrrolidinone-5-carboxylic acid, which exhibits a self-organization cooperation interaction under the coordination to RE^{3+} (Eu^{3+}, Tb^{3+}). The pure organic silica hybrids (PDCA-Si) without RE^{3+} presents the small particle size and main blue luminescence with maximum peak 462 nm occupying a broad band from 425 to 550 nm. When Eu^{3+} and Tb^{3+} are introduced, the particle size of the hybrids increases, indicating the coordination effect has influence on the microstructure of hybrids. Besides, the corresponding Eu and Tb hybrids (Eu–PDCA-Si, Tb–PDCA-Si) show the characteristic red and green luminescence of Eu^{3+} and Tb^{3+}, respectively, which suggests that the efficient intramolecular energy transfer process take place between carboxylic groups and lanthanide ions take place. The luminescence lifetimes and quantum efficiencies of them are determined and energy transfer efficiency between PDCA-Si and Eu^{3+} (Tb^{3+}) is calculated.

1. Introduction

The ambient temperature sol–gel polycondensation is a very convenient technology to prepare silica-based organic–inorganic materials [1]. The resulting materials are transparent and have good mechanical properties such as easily controlling shape, high homogeneity and purity of products [2]. The choice of the organic unit is very broad, permitting the formation of many innovative advanced materials with improved physical and chemical properties, as well as the promising applications in such fields as optics, electronics, mechanics, membranes, etc. [3]. Luminescent materials are applied in many important optic devices such as tunable lasers, displays and amplifiers for optical communication [4].

The major drawback in photoluminescence analysis is the interference caused by autofluorescence and light scattering. For this reason, over the past decade great interest has been centered on the design of luminescent complexes containing the Eu(III) and Tb(III) ions, which possess luminescence lifetimes in the micro- to millisecond range [5]. To obtain an efficient luminescent material, the ligand needs to be able to form stable complexes with the lanthanide ions, to shield the ion from deactivating molecules. What's more, the ligand needs to reinforce the energy absorbability and to transfer it to the metal ion with high efficiency, thereby overcoming the intrinsic low absorption coefficients of the metal ions. This mechanism is called the antenna effect [6]. Recently, entrapping of lanthanide complexes with β-diketones, aromatic carboxylic acids, and heterocyclic ligands in sol–gel derived host structures has been studied to improve the luminescent properties of the hybrids [7–10].

But the solubility of lanthanide complexes in the sol–gel matrix is low as a result of the low pH needed for the hydrolysis reaction [11,12]. Some methods have been put forward to overcome these solubility problems such as linking organic complexes and inorganic matrix together while shielding the lanthanide ion from the deactivating groups by a shell of organic ligands [13,14]. The covalent Si–C bonds grafting the lanthanide complexes to the silica backbone make the final production be monophasic even at a high concentration of organic complexes. So the materials' properties are improved largely and lanthanide-containing organic–inorganic hybrid materials processed by sol–gel method are considered to be good candidates to applications in optical devices.

The development of novel linkages for connecting organic compounds to inorganic solid supports is an important and active area because the choice of linker is a key consideration in designing a material since the stability of the linker limits the chemistry in the synthesis route and the final materials' properties [15]. In the former research, many researchers have paid their attentions to the modification of the siloxanes [16–25]. There are five general ways to synthesis lanthanide-centered luminescent hybrid materials: carboxyl-modification [26–28], amino-modification [29–31],

* Corresponding author. Tel.: +86 21 65984663; fax: +86 21 65982287.
E-mail address: byan@tongji.edu.cn (B. Yan).

0022-328X/$ - see front matter © 2009 Elsevier B.V. All rights reserved.
doi:10.1016/j.jorganchem.2009.03.048

hydroxyl-modification [32–36], sulfide-modification [37] and sulfonic-modification [38] etc.

Thus, our specific investigations have concerned about the synthesis of the siloxane-functionalized heterocyclic carboxylic acid as precursor of hybrids. The structure as well as the texture of the hybrid solids are also investigated that how the coordination between the ions and the ligands in the sol–gel process can impact on the organization in those amorphous systems. 2-Pyrrolidinone-5-carboxylic acid is used as the original reagent, which can react with 3-(triethoxysilyl)-propyl isocyanate and the derived organosilane precursor could complex with Eu^{3+}/Tb^{3+} ions. The pyrrolidinone unit possesses the adjacent –NH group and carboxyl group, which can produce the chelation effect after the modification of –NH. This is very important for the whole coordination interaction of the hybrid systems. Besides, the carboxyl group may take part in the coordination to stabilize the whole hybrids. They are generally performed at room temperature where gelation particles have to be stabilized by chemical cross-linking. As an alternative, we developed an oil-in-water emulsion process involving the drying gelation on a vacuum line, followed by the rapid condensation of silicates, leading to stable hybrid micro-particles. The structure of the deposited silica particles appears to depend on both organosilane concentration and the coordination interactions.

2. Experimental

2.1. Chemicals and procedures

Starting materials were purchased from Aldrich or Fluka and were used as received. All normal organic solvents were purchased from China National Medicines Group and were distilled before utilization according to the literature procedures [39]. Terbium and europium nitrates were obtained from the corresponding oxides treated by dilute nitric acid.

The typical procedures for the preparation of hybrid precursor (PDCA-Si) and hybrid material are described in the Fig. 1. 0.775 g (6 mmol) 2-pyrrolidinone-5-carboxylic acid was first dissolved in 15 mL pyridine by stirring and then 1.484 g (6 mmol) 3-(triethoxysilyl)-propyl isocyanate was added to the solution by drops. The whole mixture was refluxing at 80 °C for 4 h. The solution was condensed to evaporate the solvent and then the residue was dried on a vacuum line. A colorless oil was obtained. ^{1}H NMR ($CDC1_3$, 500 MHz) 0.68(t, 2H, H_3), 1.22(t, 9H, H_1) 1.71(m, 2H, H_4), 2.28(t, 2H, H_7), 2.45(m, 2H, H_8), 3.14(q, 2H, H_5), 3.83(q, 6H, H_2), 4.87(t, 2H, H_9), 7.02 (t, 1H, H_6), 10.0(s, 1H, H_{10}).

The sol–gel derived hybrid PDCA-Si was prepared as follows: 0.6 mmol hybrid precursor PDCA-Si and 1.2 mmol tetraethoxysilane (TEOS) were dissolved in 5 ml ethanol with stirring. The mixture was agitated magnetically to achieve a single phase in a covered Teflon beaker for 4 h, and then 30 ml water was added under gentle magnetic stirring to form an initial o/w (oil-in-water) macro-emulsion for an hour. After that, it was dried on a vacuum line at 60 °C immediately. After aged until the onset of gelation which occurred, the gels were collected for the physical properties studies.

The sol–gel derived hybrid containing lanthanide ions Eu–PDCA-Si and Tb–PDCA-Si were prepared as follows: 0.6 mmol hybrid precursor was dissolved in 5 ml ethanol with stirring. And 0.2 mmol $RE(NO_3)_3 \cdot 6H_2O$ ($Tb(NO_3)_3 \cdot 6H_2O$ and $Eu(NO_3)_3 \cdot 6H_2O$, respectively) and 1.2 mmol tetraethoxysilane (TEOS) was added into the solution, respectively. The mixture was agitated magnetically to achieve a single phase in a covered Teflon beaker for 4 h, and then 30 ml water was added under gentle magnetic stirring

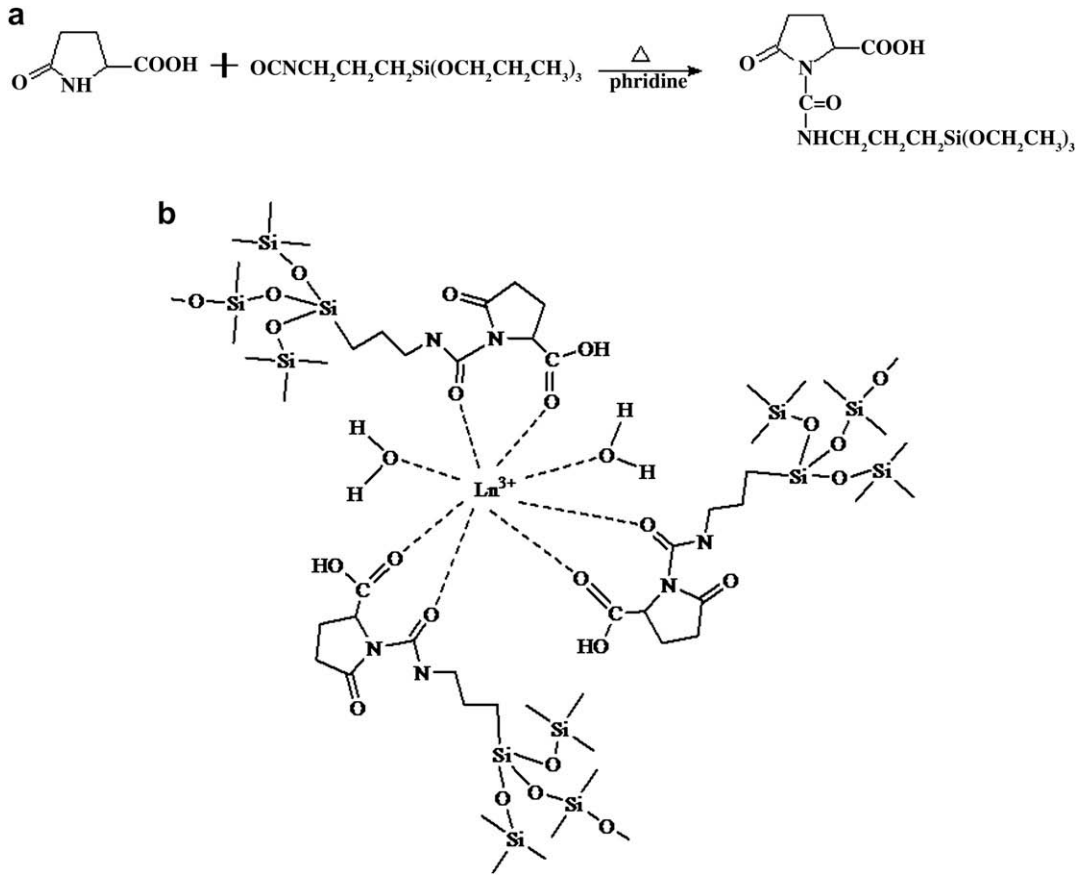

Fig. 1. The scheme for the typical procedures for the preparation of hybrid precursor PDCA-Si and the corresponding hybrids.

to form an initial o/w (oil-in-water) macro-emulsion for an hour. After that, it was dried on a vacuum line at 60 °C immediately. After aged until the onset of gelation which occurred, the gels were collected for the physical properties studies.

2.2. Measurements

Fourier transform infrared (FTIR) spectra were measured within the 4000–400 cm^{-1} region on an (Nicolet model 5SXC) infrared spectrophotometer with the KBr pellet technique. ^1H NMR (Proton Nuclear Magnetic Resonance) spectra were recorded in $CDCl_3$ on a BRUKER AVANCE-500 spectrometer with tetramethylsilane (TMS) as inter reference. Diffuse reflectance ultraviolet-visible spectra (DRUVS) of hybrid materials were recorded with a BWSpec 3.24u_42 spectrophotometer. Luminescence (excitation and emission) spectra of these solid complexes were determined with a RF-5301 spectrophotometer whose excitation and emission slits were 5 and 3 nm, respectively. And the fluorescence decay properties were recorded on an Edinburgh Analytical Instruments. The X-ray diffraction (XRD) measurements were carried out on powdered samples via a "BRUKER D8" diffractometer (40 mA_40 kV) using monochromated Cu Kα1 radiation (λ = 1.54 Å) over the 2θ range of 10–70°. Scanning electronic microscope (SEM) images were obtained with a Philps XL-30. The quantum yield of were determined using an integrating sphere (150 mm diameter, $BaSO_4$ coating) of Edinburgh Instruments. The spectra were corrected. The quantum yield can be defined as the integrated intensity of the luminescence signal divided by the integrated intensity of the absorption signal. Only the intense luminescence band of the $^5D_0 \rightarrow {}^7F_2$ transition around 612 nm was measured by the integrating sphere, but this intensity value was corrected by taking into account the relative intensity of the other transitions (as determined from the steady-state luminescence spectrum in the 550–750 nm region). In this way, an intensity value that corresponds to the total luminescence output was obtained. The absorption intensity was calculated by subtracting the integrated intensity of the light source with the sample in the integrating sphere, from the integrated intensity of the light source with a blank sample in the integrating sphere.

3. Results and discussion

3.1. Characterization of composition and microstructure

The Fourier transform infrared (FTIR) spectra for PDCA (a), the precursor PDCA-Si (b), hybrid materials PDCA-Si (c) and Tb–PDCA-Si (d) are shown in Fig. 2. The peak at 3420–3306 cm^{-1} in curve of 2-pyrrolidinone-5-carboxylic acid Fig. 2a is the unique vibration of NH group. The broad peak at 3064–2817 cm^{-1} in curve of 2-pyrrolidinone-5-carboxylic acid (a) is the coupling of two carboxyl groups and it turned into broad peak of ν (O–H) at 3454 cm^{-1} in curve of precursor Fig. 2b. Two adjacent sharp peaks at 2929 cm^{-1} and 2872 cm^{-1} in curve of precursors Fig. 2b are $\nu_{as}(CH_2)$ and $\nu_s(CH_2)$ of the long carbon chain in precursors [40]. And ^1H NMR spectra relative to the precursors are in full agreement with the proposed structures. In the spectra of hybrid materials (PDCA-Si and Tb–PDCA-Si), the spectra are dominated by the ν (O–H) at 3454 cm^{-1} and ν (Si–O–Si) absorption bands at 1120–1000 cm^{-1}. The ν (O–H) came from the absorbed water in the hy-

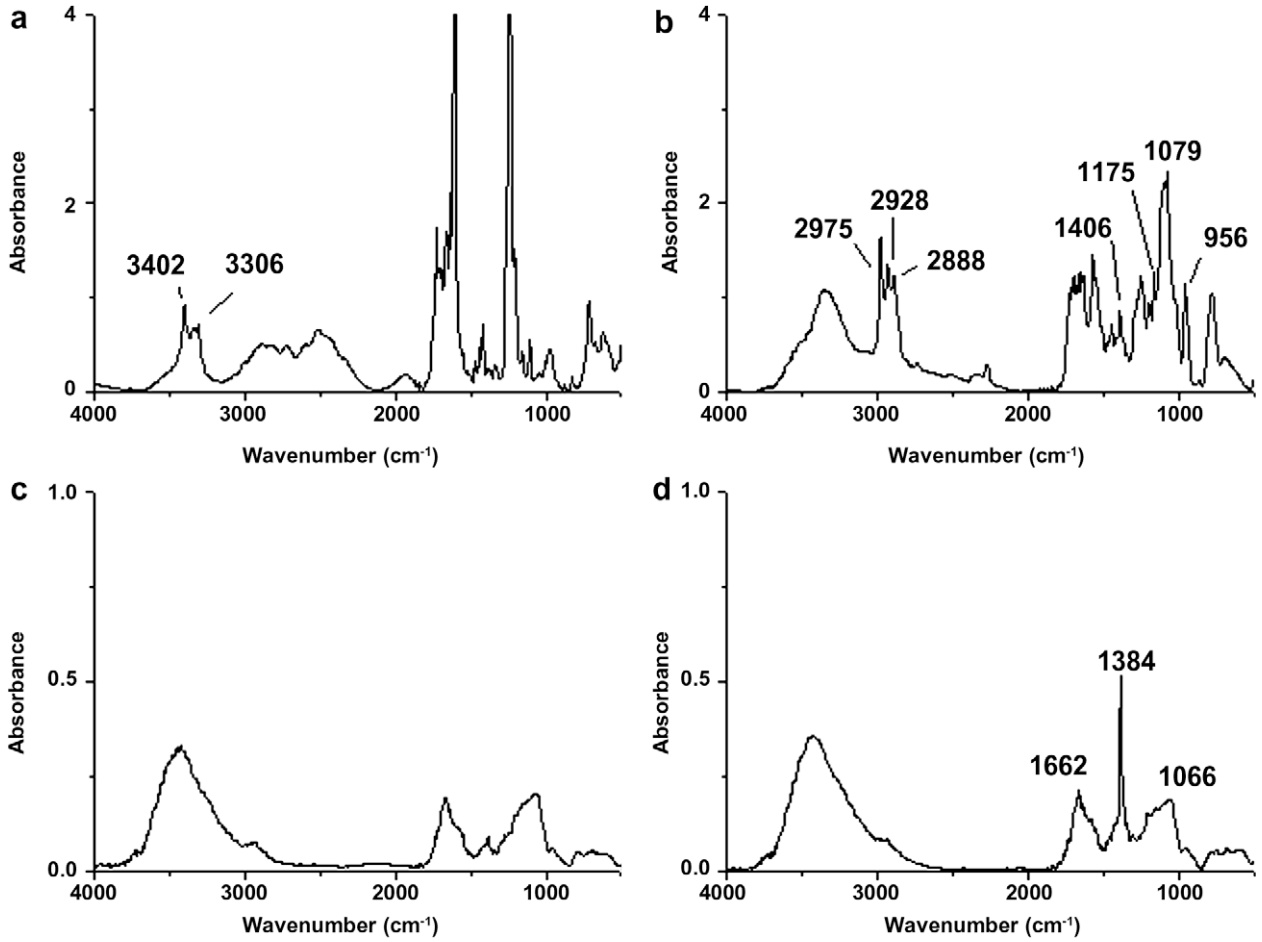

Fig. 2. Infrared spectra of PDCA (a), the precursor PDCA-Si (b), hybrid material PDCA-Si (c) and hybrid material Tb–PDCA-Si (d).

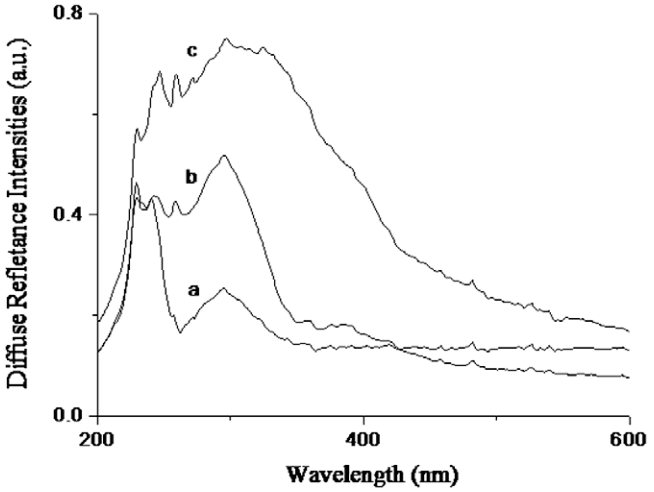

Fig. 3. Selected diffuse reflectance ultraviolet-visible spectra (DRUVS) of PDCA (a), PDCA-Si (b) and Tb–PDCA-Si (c).

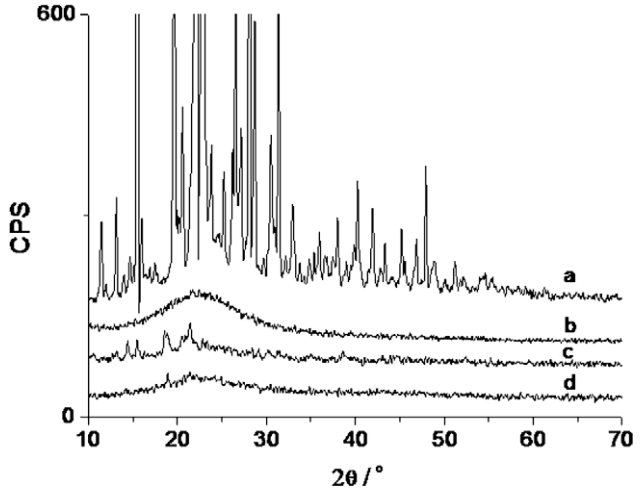

Fig. 4. The X-ray diffraction graphs of PDCA (a), PDCA-Si (b) and Tb–PDCA-Si (c) and $Tb(NO_3)_3 \cdot 6H_2O$/PDCA-Si (d) hybrid materials.

brid material. The ν (Si–C) vibration located in the 1175 cm^{-1} in IR spectra of hybrid materials (see Fig. 2) was consistent with the fact that no (Si–C) bond cleavage occurred during modification, hydrolysis and condensation reactions [26–28]. The broad absorption band at 1120–1000 cm^{-1} (ν (Si–O–Si)) indicated the formation of siloxane bonds [40]. The decrease of other peaks' intensities may be due to the containing of the organic groups by the silicate inorganic host which occurred in the hydrolysis and condensation process. Coordination of lanthanide ions by the ligands is clearly shown by infrared spectroscopy. In spectrum of precursors Fig. 2b, the ν $(COO^-)_{as}$ vibrations is located at 1650–1550 cm^{-1} and the ν $(COO^-)_{sy}$ vibrations is located at 1406 cm^{-1}. But in the spectrum of Fig. 2d, the ν $(COO^-)_{sy}$ vibration is shifted to the 1384 cm^{-1}. The shift is a proof of the coordination of the carboxylic group to the metallic ion with the oxygen atoms [26–28].

Fig. 3 shows the diffuse reflectance ultraviolet-visible spectra (DRUVS) of PDCA (a), hybrid material PDCA-Si (b) and hybrid material Tb–PDCA-Si (c). In the spectra, the absorption peak around 290 nm corresponded to the $n \rightarrow \pi^*$ electronic transition of carboxylic group [26–28]. The increase of intensities from 280 nm to 322 nm corresponds to the coordination of carbonyl oxygen to lanthanide ions. The broad absorption band is favorable for the energy transfer and luminescence of Eu or Tb ions.

The X-ray diffraction graphs of PDCA (a), hybrid material PDCA-Si (b) and hybrid material Tb–PDCA-Si (c) and hybrid material $Tb(NO_3)_3 \cdot 6H_2O$/PDCA-Si (PDCA-Si doped with terbium nitrates) (d) are shown in Fig. 4. In the spectrum of PDCA (a), there are characteristic X-radiation peaks of 2-pyrrolidinone-5-carboxylic acid crystals. But the diffractogram of hybrid materials reveals that all of the hybrid materials with $10^\circ \leqslant n \leqslant 70^\circ$ are mostly amorphous. To hybrid material PDCA-Si (b), it is totally amorphous and dominated by a broad peak centered 22°. However, in the Hybrid material Tb–PDCA-Si (c) there are some narrow peaks protrude from the baseline which are attributed to the regular arrangement of the organic groups. This is consistent with the suggestion of coordination interactions between lanthanide ions and carboxylic acid groups which was proved previously. To exclude the impact of lanthanide nitrates, hybrid material I simply doped with Terbium nitrates according to the ratio of previous experiment description of hybrid material $Tb(NO_3)_3 \cdot 6H_2O$/PDCA-Si are prepared and its XRD spectrum (d) is measured. From the spectra (d), the intensities of broad peak still exists which means that simply mix could not eliminate the broad peak. Comparing (c) and (d), the difference proved the coordination between the lanthanide ions and ligands.

The scanning electron micrographs (SEM) of these hybrid materials can give some proofs from the texture. In Fig. 5, left graph is hybrid material PDCA-Si and right graph is hybrid material Tb–PDCA-Si. These are mostly owing to the adapting sol–gel treatment. In the sol process, the o/w macro-emulsion is decisive and responsibility for the materials' final texture. The difference between two hybrids is the scale of two kinds of particles and it can be resolved easily. In hybrid material PDCA-Si, because of the hydrogen-bond, organic groups aggregated. In the hybrid material Tb–PDCA-Si, the coordination between organic groups and lanthanide ions disturbed the regular arrangement of the organic moieties so the particle scale of the hybrid material Tb–PDCA-Si is smaller than that of the hybrid material PDCA-Si. Carboxylic acids are already well-known to be good chelating groups to sensitize luminescence of lanthanide ions [7]. The mechanism usually described for sensitized emission in lanthanide complexes proceeds through the following steps. At the first, the ligands absorb energy via a ground singlet-excited singlet transition. Then the energy takes lossless intersystem crossing process to transfer from the excited singlet to the triplet state. After the energy transfer from the excited state of ligands to the emissive state of rare earth ions, the characteristic emission of the excited lanthanide ions can be observed.

This hybrid material system presents a number of advantages: (i) the hybrid particles exhibit a micrometric structure, and not a continuous hybrid network, so that they are convenient to use and need not to be ground; (ii) the synthesis does not involve any high temperature process and the time needed is shortened. In this study, it has been shown that the modification is practical and the obtained hybrid materials possess good physical properties. As one synthesis method, it can be easily applied to other organic compounds and to different modified alkoxysilanes. Furthermore, the current molecular design method can be conveniently applied to other hybrid systems. The desired properties can be tailored by an appropriate choice of the precursors. So this kind of molecular-based hybrid material can be expected to be a promising candidate for tailoring desired properties to the host in many fields of applications.

3.2. Photophysical properties

The luminescence behaviors of all of the materials have been investigated at 298 K by direct excitation of the ligands (290 nm). Representative emission spectra are given in Figs. 6–8, respectively. Fig. 6 illustrates typical photoluminescence spectra of the

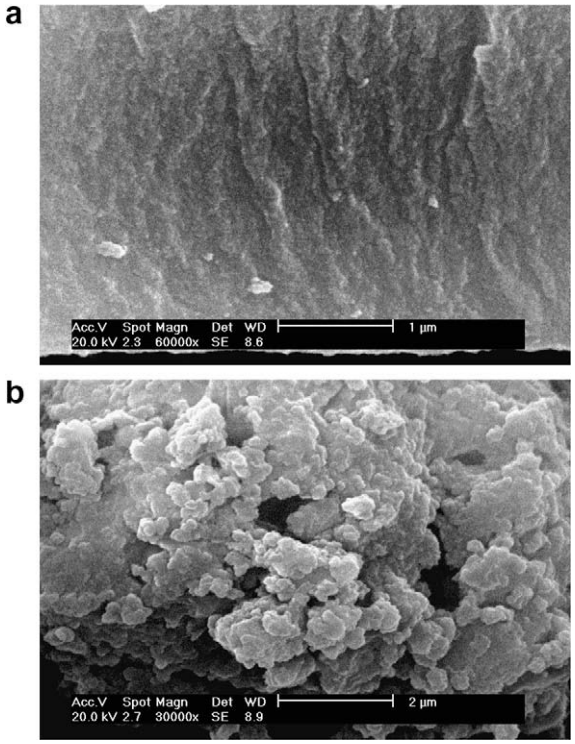

Fig. 5. The selected scanning electron micrographs of the hybrid material: (a) PDCA-Si and (b) Tb–PDCA-Si.

hybrid material PDCA-Si. Because no lanthanide ions are introduced in them, this kind of hybrid materials can only emit the luminescence of the organic group. The peak of the emission is located at 460 nm. Fig. 7 illustrates typical photoluminescence spectra of the europium hybrid material Eu–PDCA-Si. The maxima of these bands are at 590 and 613 nm which is associated with $^5D_0 \rightarrow {}^7F_1$ and $^5D_0 \rightarrow {}^7F_2$ transitions, respectively. The energy transfer from the carboxylic ligand to europium (III) is not perfect, as can be noticed to the residual ligand emission from 500 to 570 nm. A prominent feature that may be noted in these spectra is the high intensity ratios of $I(^5D_0 \rightarrow {}^7F_2)/I(^5D_0 \rightarrow {}^7F_1)$. The intensity (the integration of the luminescent band) ratio of the $^5D_0 \rightarrow {}^7F_2$ transition to $^5D_0 \rightarrow {}^7F_1$ transition has been widely used as an indicator of Eu^{3+} site symmetry [41]. $^5D_0 \rightarrow {}^7F_1$ transition is

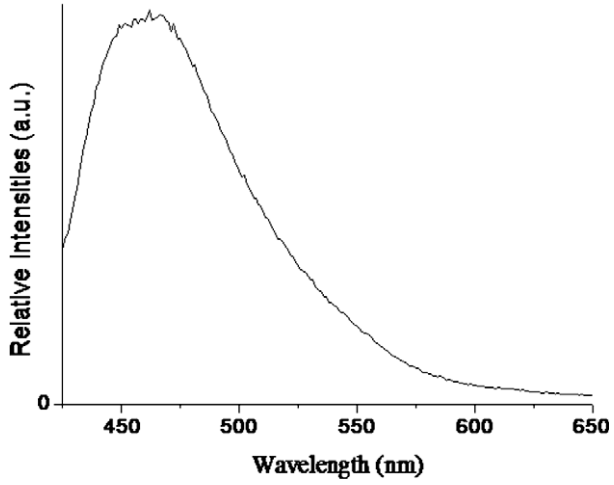

Fig. 6. The emission spectra of hybrid material PDCA-Si.

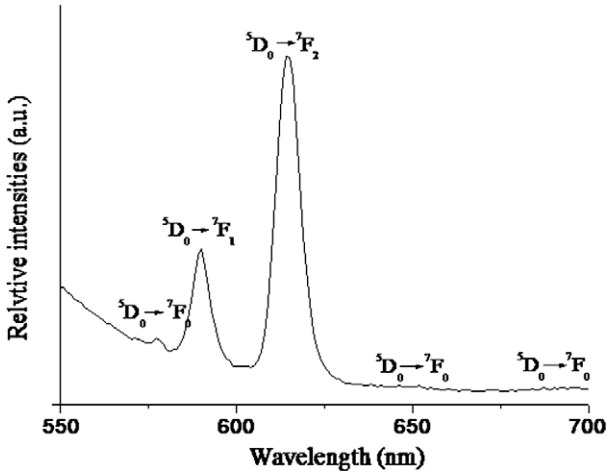

Fig. 7. The emission spectra of the hybrid material Eu–PDCA-Si.

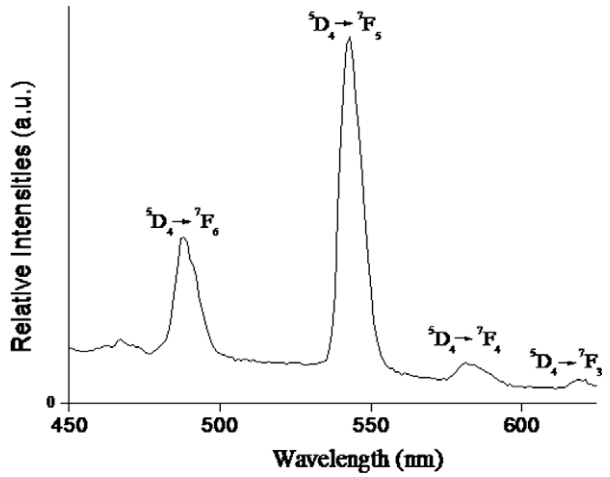

Fig. 8. The emission spectra of the hybrid material Tb–PDCA-Si.

magnetic-dipolar transitions and insensitive to their local structure environment while $^5D_0 \rightarrow {}^7F_2$ transition is electric-dipolar transitions and sensitive to the coordination environment of the Eu^{3+} ion. When the interactions of the rare-earth complex with its local chemical environment are stronger, the complex becomes more nonsymmetrical and the intensity of the electric-dipolar transitions becomes more intense. As a result, $^5D_0 \rightarrow {}^7F_1$ transition (magnetic-dipolar transitions) decreased and $^5D_0 \rightarrow {}^7F_2$ transition (electric-dipolar transitions) increased. In this situation, the intensity ratios are approximately 4.5. This ratio is only possible when the europium ion does not occupy a site with inversion symmetry [42]. It is clear that the strong coordination interactions took place between the organic groups and lanthanide ions. Fig. 8 illustrates typical photoluminescence spectra of the terbium hybrid material Tb–PDCA-Si. Narrow-width emission bands with maxima at 487, 543, 580 and 619 nm are recorded. These bands are related to the transition from the triplet state energy level of Tb^{3+} to the different single state levels and are attributed to the $^5D_4 \rightarrow {}^7F_6$, $^5D_4 \rightarrow {}^7F_5$, $^5D_4 \rightarrow {}^7F_4$ and $^5D_4 \rightarrow {}^7F_3$ transitions of Tb^{3+} ions, respectively. And the efficiency is higher than that from the carboxylic group to Eu^{3+} ion.

The luminescence decays of the hybrid material fit a single-exponential rule ($\text{Fit} = A + B_1{}^* \exp(-t/T_1)$), confirming that all lanthanide ions lie in the same coordination environment. The resulting lifetime of the europium and terbium hybrids is 0.74 ms and

0.81 ms, respectively. What's more, it appears as a general trend that the lifetimes in this hybrid materials are similar as those in the corresponding organic complexes which range is from 0.2 to 1.7 ms [43], indicating an important maintenance of luminescent stability for the covalently bonded molecular network in the hybrid systems. The resulting lifetime data of Eu and hybrids were given in Table 1. The luminescent lifetime of terbium hybrids is longer than that of europium ones, which is the similar order to the luminescent intensity, indicating both PDCA-Si show the more suitable for the luminescence of Tb^{3+} than Eu^{3+}.

Furtherly, we selectively determined the emission quantum efficiencies of the $^5D_0$ excited state of europium ion for Eu^{3+} hybrids on the basis of the emission spectra and lifetimes of the $^5D_0$ emitting level, the detailed luminescent data were shown in Table 1. The quantum efficiency of the luminescence step, η expresses how well the radiative processes (characterized by rate constant A_r) compete with non-radiative processes (rate constant A_{nr}) [44–52]:

$$\eta = A_r/(A_r + A_{nr}) \quad (1)$$

Non-radiative processes influence the experimental luminescence lifetime (τ_{exp}) by the equation [43–51]

$$\tau_{exp} = (A_r + A_{nr})^{-1} \quad (2)$$

So quantum efficiency (η) can be calculated from radiative transition rate constant and experimental luminescence lifetime from the following equation [44–52]:

$$\eta = A_r \tau_{exp} \quad (3)$$

where A_r can be obtained by summing over the radiative rates for each $^5D_0 \rightarrow {}^7F_J$ transitions of Eu^{3+} [44–52]

$$A_r = \sum A_{0J} = A_{00} + A_{01} + A_{02} + A_{03} + A_{04} \quad (4)$$

$$A_{0J} = A_{01}(I_{0J}/I_{01})(\upsilon_{01}/\upsilon_{0J}) \quad (5)$$

Here A_{0J} is the experimental coefficients of spontaneous emissions, among A_{01} is the Einstein's coefficient of spontaneous emission between the $^5D_0$ and $^7F_1$ energy levels, which can be determined to be 50 s^{-1} approximately [48] and as a reference to calculate the value of other A_{0J}. I is the emission intensity and can be taken as the integrated intensity of the $^5D_0 \rightarrow {}^7F_J$ emission bands [45,46]. υ_{0J} refers to the energy barrier and can be determined from the emission bands of Eu^{3+}'s $^5D_0 \rightarrow {}^7F_J$ emission transitions. The branching ratio for the $^5D_0 \rightarrow {}^7F_{5,6}$ transitions can be neglected as they both are not detected experimentally, whose influence can be ignored in the depopulation of the $^5D_0$ excited state [44–52]. Since $^5D_0 \rightarrow {}^7F_1$ belongs to the isolated magnetic dipole transition, it is practically independent of the chemical environments around the Eu^{3+} ion, and thus can be considered as an internal reference for the whole spectrum, the experimental coefficients of spontaneous emission, A_{0J} can be calculated according to the equation [44–52]. Here the emission intensity, I, taken as integrated intensity S of the $^5D_0 \rightarrow {}^7F_{0\text{-}4}$ emission curves, can be defined as below:

$$I_{i-j} = \hbar\omega_{i-j}A_{i-j}N_i \approx S_{i-j} \quad (6)$$

where i and j are the initial ($^5D_0$) and final levels ($^7F_{0\text{-}4}$), respectively, ω_{i-j} is the transition energy, A_{i-j} is the Einstein's coefficient of spontaneous emission, and N_i is the population of the $^5D_0$ emitting level.

On the basis of the above discussion, the quantum efficiency of the europium hybrids can be determined as 15%, which is higher than the absolute quantum efficiency (11%) from experimental measurement, which reveals that there exist some errors for the spectrum and lifetimes. From the equation of η, it can be seen the value η mainly depends on the values of two quantum: one is lifetimes and the other is I_{02}/I_{01} (red/orange ratio). If the lifetimes and red/orange ratio are large, the quantum efficiency must be high. Comparing the value of luminescent quantum efficiencies, it can be found that they show the similar rule to the value of luminescent lifetimes. The luminescent quantum efficiency of terbium hybrids is higher than that of europium one, suggesting the fact of different energy match and intramolecular energy transfer process. Besides, the three different color hybrids (PDCA-Si, Eu–PDCA-Si and Tb–PDCA-Si) possess the same order of luminescent efficiency, which can be expected to achieve the white luminescence from the suitable composition of the three hybrid components. The deep research to modify the composition ratio of the three luminescent species (blue, green and red luminescent component) to obtain the white luminescent is underway.

In order to study the coordination environment surround lanthanide ions especially the influence caused by vibrations of water molecules, according to Horrocks' previous research [53,54], it is therefore expected that probable number of coordinated water molecules (n_w) can be calculated as following equation:

$$n_w = 1.05(A_{exp} - A_{rad}) \quad (7)$$

Based on the results, the coordination number of water molecules (Eu containing hybrid materials) can be estimated to be about 1.5. The coordination water molecules produce the severe vibration of hydroxyl group, resulting in the large non-radiative transition and decreasing the luminescent efficiency.

At last, we can predict the energy transfer efficiencies (η_{ET}) of the two covalently bonded lanthanide hybrid materials [55,56]

$$\eta_{ET} = 1 - \eta_{DA}/\eta_D \quad (8)$$

Here η_{DA}, η_D represent the quantum efficiencies of coexistent energy-donor and individual donor, respectively. For Eu–PDCA-Si and Tb–PDCA-Si (η_{DA}), PDCA-Si can be considered as the host and the energy donor for Eu^{3+} or Tb^{3+} (energy acceptor, η_D). On the basis of the references [55,56], the energy transfer efficiency from PDCA-Si to Eu^{3+} in Eu–PDCA-Si hybrids (39%) is lower than that between PDCA-Si and Tb^{3+} in Tb–PDCA-Si hybrids (75%). The higher energy transfer efficiency for Tb hybrids leads to the higher luminescent quantum efficiency.

Table 1
Photoluminescent data of all hybrid materials.

Hybrids	PDCA-Si	Eu–PDCA-Si	Tb–PDCA-Si
I_{02}/I_{01}	–	10.01	–
τ (ms)	–	0.54[a]	0.81[b]
$1/\tau$ (s^{-1})	–	1850	–
A_r (s^{-1})	–	280	–
A_{nr} (s^{-1})	–	1570	–
n_w	–	~1.5	–
η (%)	28	11 (15[c])	21
η_{ET} (%)	–	39	75

[a] For $^5D_0 \rightarrow {}^7F_2$ transition of Eu^{3+}.
[b] For $^5D_4 \rightarrow {}^7F_5$ transition of Tb^{3+}.
[c] Luminescent quantum efficiency from the determination with luminescent spectrum and lifetime.

4. Conclusions

In summary, a new kind of luminescent hybrid molecular-based materials have been achieved by an adapting traditional sol–gel method based on an o/w process and organosilane polycondensation. One molecule bridge PDCA-Si is designed and then three covalently bonded hybrid materials exhibiting three multi-color luminescence (blue for PDCA-Si, green for Tb–PDCA-Si and red for Eu–PDCA-Si) were constructed through the coordination to europium or terbium ions. Especially the quantum efficiency and

energy transfer efficiency of Tb hybrids are higher than those of Eu one.

Acknowledgements

This work was supported by the National Natural Science Foundation of China (20671072) and Program for New Century Excellent Talents in University (NCET 2008).

References

[1] D.A. Loy, K.J. Shea, Chem. Rev. 95 (1995) 1431–1442.
[2] U. Schubert, N. Husing, A. Lorenz, Chem. Mater. 7 (1995) 2010–2027.
[3] C. Sanchez, G.J.D.A. Sloer-Illia, F. Ribot, T. Lalot, C.R. Mayer, V. Cabuil, Chem. Mater. 13 (2001) 2083–3061.
[4] G. Blass, B.C. Grabmaier, Luminescent Materials, Springer, Berlin, 1994.
[5] L. Prodi, S. Pivari, F. Bolletta, M. Hissler, R. Ziessel, Eur. J. Inorg. Chem. (1998) 1959–1965.
[6] G. Crosby, R.E. Whan, R. Alire, J. Chem. Phys. 34 (1961) 743–749.
[7] L.R. Matthews, E.T. Knobbe, Chem. Mater. 5 (1993) 1697–1702.
[8] B. Yan, H.J. Zhang, J.Z. Ni, Mater. Sci. Eng. B 52 (1998) 123–128.
[9] Y. Zhang, M.Q. Wang, J. Xu, J. Mater. Sci. Eng. B 47 (1997) 23–27.
[10] B. Yan, Mater. Lett. 57 (2003) 2535–2539.
[11] K. Driesen, C. Gorller-Walrand, K. Binnemans, Mater. Sci. Eng. C 18 (2001) 255–258.
[12] K. Driesen, F. Lenaerts, K. Binnemans, C. Gorller-Walrand, Phys. Chem. Chem. Phys. 4 (2002) 552–555.
[13] C. Sanchez, F. Ribot, New J. Chem. 18 (1994) 1007–1047.
[14] B. Viana, N. Koslova, P. Aschehoug, C. Sanchez, J. Mater. Chem. 5 (1995) 719–724.
[15] I.W. James, Tetrahedron 55 (1999) 4855–4946.
[16] M. Schmider, E. Muh, J.E. Klee, R. Mulhaupt, Macromolecules 38 (2005) 9548–9555.
[17] D. Hu, C. Croutxe-Barghorn, M. Feuillade, C. Carre, J. Phys. Chem. B 109 (2005) 15214–15220.
[18] H.R. Li, J. Lin, H.J. Zhang, L.S. Fu, Chem. Mater. 14 (2002) 3651–3655.
[19] D.W. Dong, S.C. Jiang, Y.F. Men, X.L. Ji, B.Z. Jiang, Adv. Mater. 12 (2000) 646–649.
[20] A.C. Franville, D. Zambon, R. Mahiou, Chem. Mater. 12 (2000) 428–435.
[21] B. Yan, F.F. Wang, J. Organomet. Chem. 692 (2007) 2395–2401.
[22] R.A. Sa Ferreira, L.D. Carlos, R.R. Goncalves, S.J.L. Ribeiro, V.D. Bermudez, Chem. Mater. 13 (2001) 2991–2998.
[23] L.D. Carlos, R.A. Sa Ferreira, R.N. Pereira, M. Assuncao, V.D. Bermudez, J. Phys. Chem. B 108 (2004) 14924–14932.
[24] L.D. Carlos, Adv. Funct. Mater. 12 (2002) 819–823.
[25] A. Quach, V. Escax, L. Nicole, P. Goldner, O. Guillot-Noel, P. Aschehoug, P. Hesemann, J. Moreau, D. Gourier, C. Sanchez, J. Mater. Chem. 17 (2007) 2552–2560.
[26] Q.M. Wang, B. Yan, Cryst. Growth Des. 5 (2005) 497–503.
[27] Q.M. Wang, B. Yan, J. Mater. Res. 20 (2005) 592–598.
[28] Q.M. Wang, B. Yan, J. Photochem. Photobiol. A: Chem. 175 (2005) 159–165.
[29] Q.M. Wang, B. Yan, J. Mater. Chem. 14 (2004) 2450–2455.
[30] Q.M. Wang, B. Yan, J. Photochem. Photobiol. A: Chem. 178 (2006) 70–75.
[31] B. Yan, B. Zhou, Q.M. Wang, J. Lumin. 126 (2007) 556–560.
[32] Q.M. Wang, B. Yan, J. Organomet. Chem. 691 (2006) 540–545.
[33] Q.M. Wang, B. Yan, J. Organomet. Chem. 691 (2006) 3567–3573.
[34] B. Yan, D.J. Ma, J. Solid State Chem. 179 (2006) 2059–2066.
[35] B. Yan, X.F. Qiao, Photochem. Photobiol. 83 (2007) 971–978.
[36] B. Yan, H.F. Lu, J. Non-Cryst. Solids 352 (2006) 5331–5335.
[37] B. Yan, H.F. Lu, Inorg. Chem. 47 (2008) 5601–5610.
[38] D.D. Perrin, W.L.F. Armarego, D.R. Perrin, Purification of Laboratory Chemicals, Pergamon Press, Oxford, 1980.
[39] F. Pretsch, P. Buhlmann, C. Affolter, Structure Determination of Organic Compounds, Springer, Berlin, 2003. 2nd printing.
[40] Z. Wang, J. Wang, H.J. Zhang, Mater. Chem. Phys. 87 (2004) 44–48.
[41] Y. Hasegawa, M. Yamamuro, Y. Wada, N. Kanehisa, Y. Kai, S. Yanagida, J. Phys. Chem. A 107 (2003) 1697–1702.
[42] C.G. Gulgas, T.M. Reineke, Inorg. Chem. 44 (2005) 9829–9836.
[43] O.L. Malta, H.F. Brito, J.F.S. Menezes, F.R.G.E. Silva, S. Alves, F.S. Farias, A.V.M. deAndrade, J. Lumin. 75 (1997) 255–268.
[44] M.H.V. Werts, R.T.F. Jukes, J.W. Verhoeven, Phys. Chem. Chem. Phys. 4 (2002) 1542–1548.
[45] C.Y. Peng, H.J. Zhang, J.B. Yu, Q.G. Meng, L.S. Fu, H.R. Li, L.N. Sun, X.M. Guo, J. Phys. Chem. B 109 (2005) 15278–15287.
[46] L.D. Carlos, Y. Messaddeq, H.F. Brito, Adv. Mater. 12 (2000) 594–598.
[47] E.E.S. Teotonio, J.G.P. Espinola, H.F. Brito, O.L. Malta, S.F. Oliveria, D.L.A. de Faria, C.M.S. Izumi, Polyhedron 21 (2002) 1837–1844.
[48] O.L. Malta, M.A.C. dosSantos, L.C. Thompson, N.K. Ito, J. Lumin. 69 (1996) 77–84.
[49] G.F. de Sa, O.L. Malta, C.D. Donega, A.M. Simas, R.L. Longo, P.A. Santa-Cruz, E.F. da Silva, Coord. Chem. Rev. 196 (2000) 165–195.
[50] J.C. Boyer, F. Vetrone, J.A. Capobianco, A. Speghini, M. Bettinelli, J. Phys. Chem. B 108 (2004) 20137–20143.
[51] C.A. Kodaira, A. Claudia, H.F. Brito, M.C.F.C. Felinto, J. Solid State Chem. 171 (2003) 401–407.
[52] K. Binnemans, K. Van Herck, C. Gorller-Walrand, Chem. Phys. Lett. 266 (1997) 297–302.
[53] W. De, W. Horrocks, D.R. Sudnick, J. Am. Chem. Soc. 101 (1979) 334–340.
[54] W. De, W. Horrocks, D.R. Sudnick, Acc. Chem. Res. 14 (1981) 384–392.
[55] P.R. Biju, G. Jose, V. Thomas, V.P.N. Nampoori, N.V. Unnikrishnan, Opt. Mater. 24 (2004) 671–677.
[56] P.P. Lima, S.S. Nobre, R.O. Freire, S.A. Junior, L. Mafra, J. Phys. Chem. C 111 (2007) 17627–17634.